Available online at www.sciencedirect.com
ScienceDirect
Ceramics International 37 (2011) 533–541
CERAMICS INTERNATIONAL
www.elsevier.com/locate/ceramint

Mechanical activation of fly ash: Effect on reaction, structure and properties of resulting geopolymer

Sanjay Kumar *, Rakesh Kumar

National Metallurgical Laboratory, Council of Scientific and Industrial Research, Jamshedpur 831007, India

Received 9 July 2010; received in revised form 26 July 2010; accepted 22 September 2010
Available online 28 October 2010

Abstract

Geopolymerisation of mechanically activated fly ash was studied at ambient (27 °C) and elevated (60 °C) temperatures by isothermal conduction calorimeter. Under both the conditions, mechanical activation enhanced the rate and decreased time of reaction. It was interesting to observe that in the samples milled for 45 min (median size ~5 μm), a broad peak corresponding to geopolymerisation initiated at 27 °C after 32 h. The rate maxima at 60 °C, a measure of fly ash reactivity, showed a non-linear dependence on particle size and increased rapidly when the median size was reduced to less than 5–7 μm. Improvement in strength properties is correlated with median particle size, and reactivity of fly ash. The characterisation of the geopolymer samples by SEM-EDS, XRD and FTIR revealed that mechanical activation leads to microstructure and structural variations which can be invoked to explain the variation in the properties.

Keywords: B. Microstructure-final; C. Strength; Fly ash; Mechanical activation; Reactivity; Geopolymerisation

1. Introduction

Geopolymers are new class of synthetic alumino-silicate materials formed due to reaction between alumino-silicates and oxides with alkaline media [1]. Due to easy, energy efficient, ecofriendly processing and excellent mechanical properties, geopolymers are fast emerging materials of choice for a range of construction and building materials, fire resistance ceramics, composites, matrix for immobilization of toxic wastes, precursor for monolithic and many others. A large number of naturally occurring and industrially produced alumino-silicate solids are used for geopolymer synthesis [2–5]. Recently there has been a growing trend to use fly ash in geopolymers due to their easy availability, good workability during processing and improved durability in final product [6–12]. The limiting factor which has hindered the use of fly ash in geopolymers is its low reactivity. In geopolymers, the reactivity of fly ash depends on its particle size, glass content and glass composition [10,13]. The low reactivity of fly ash leads to slow setting and early strength development. In many cases the dissolution of fly ash is not complete before the final hardened structure is formed [14].

The merit of using mechanical activation (MA) for improving bulk and surface reactivity is well accepted. MA offers the possibility to alter the reactivity of solids through physicochemical changes in bulk and surface without altering overall chemistry of the material [15–17]. Some very interesting finding on the MA of blast furnace slag and fly ash has been recently reported by us [18–21]. Complete hydration of slag can be achieved for mechanically activated slag and without any chemical addition [18,19]. Mechanical induced reactivity of fly has been exploited to tailor properties of geopolymer, and geopolymer having compressive strength of up to 120 MPa can be produced through judicious application of MA along with other processing parameters [20–22].

It was earlier reported by us that the selection of milling device for MA influences the reactivity of fly ash, i.e. fly ash of same fineness behaves differently depending upon milling device [20,21]. Geopolymer prepared from fly ash that was mechanically activated in a vibratory mill showed superior mechanical properties as compared to their counterparts prepared from fly ash of similar particle size but obtained

* Corresponding author at: MEF Division, National Metallurgical Laboratory, Council of Scientific & Industrial Research, Jamshedpur 831007, India. Tel.: +91 657 2345049/9939326346; fax: +91 657 2345153.
E-mail addresses: sanjay_kumar_nml@yahoo.com, sunju@nmlindia.org (S. Kumar).

0272-8842/$36.00
doi:10.1016/j.ceramint.2010.09.038

using other high energy mills, e.g. attrition mill [20]. Recently, suitability of vibratory mill for MA of fly ash for application in geopolymer concrete has also been reported by other researchers [22].

The objective of the present investigation was to carry out a systematic study on the geopolymerisation behaviour of fly ash that was mechanically activated in an eccentric vibratory mill (EVM) for different duration. The effect of mechanical activation on reaction, structure and properties of geopolymers was elucidated using isothermal conduction calorimeter, Fourier transform infrared spectroscopy (FTIR), X-ray diffractometry (XRD), scanning electron microscopy (SEM) and evaluation of physical properties. Attempt has been made to correlate the reaction with structure and properties.

2. Experimental

The fly ash was collected from a Thermal power plant in Chhattisgarh, India. The chemical analysis and physical properties of the fly ash are given in Table 1. The glass content of the fly ash was determined by counting the grains in a polarising microscope using the method described in Indian Standard IS 12089:1987. Mechanical activation of fly ash was carried out in laboratory size EVM (SIEBTECHNIK, ESM 234, Germany). 2 kg batch size was used for milling. The size of stainless steel media balls was 12.5 mm. Material to media ratio of 1:35 was maintained during milling. The fly ash was milled for 5, 10, 20, 30, 45, 60 and 90 min, and the milled samples are referred to as FA5, FA10, . . ., FA90 in subsequent description. Raw fly ash (FA0) was used as a reference.

The particle size analysis of raw and milled fly ash was carried out using laser particle size analyser (MASTERSIZER S, Malvern, UK). The specific surface area was measured using MICROMERITICS (USA) specific surface area analyser (Model ASAP2020). The rate of heat evolution during the reaction (dq/dt) was measured using an eight channel isothermal conduction calorimeter (TAM AIR, Thermometric AB, Jarafalla, Sweden). The sample preparation involved the following steps: (a) preparation of alkaline activator solution, (b) mixing of alkaline activator with the powder sample, and (c) loading of the mix in calorimeter. Analytical grade sodium hydroxide in flaky form (98% purity) was used to prepare alkaline activator solution. Alkaline activator of 6 M concentration was prepared in distilled water at least 24 h before use. 7 g solid sample and 3.5 ml of activator solution were used throughout the study. The samples were mixed outside and then loaded into the calorimeter. Calorimetric studies were carried out at 27 °C and 60 °C. The results obtained were presented in offset mode. Fourier transform infrared spectroscopy ((FT-IR-410 JASCO, U.S.A.) was used for structural characterisation of geopolymers. IR samples were prepared by mixing with KBr.

XRD patterns were recorded on a SIEMENS X-ray diffractometer (Model D500), using Co$K_{\propto}$ radiation with a Fe-filter. The scanning speed of 1°/min was used and the samples were scanned from 10° to 60° 2θ angle. Morphological characterisation of the fractured samples was done by a scanning electron microscope (JEOL SEM 840A) fitted with a Kevex energy dispersive spectrometer (EDS) for X-ray micro-analysis after carbon coating on the fractured surface. The X-ray micro-analysis of areas of interest was determined from the average of minimum six analyses and used to calculate elemental ratios.

For all the physical testing, liquid (alkali solution) to solid ratio was 0.35. The samples were prepared at 27 ± 2 °C and under relative humidity of 65%. The time difference between initial and final setting time was very small and in some cases negligible thus only initial setting time was determined by using Vicat Apparatus (AIMIL, India) on a consistent paste. For compressive strength 7 cm × 7 cm × 7 cm cubic samples were prepared by vibro-casting of geopolymer paste. Compressive strength was tested on an Automatic Compression Testing Machine (AIMIL COMPTEST 2000, India). Two sets of samples were tested: (a) samples cast and cured at 27 °C for 28 days, and (b) samples cast and cured at 27 °C for 24 h followed by curing at 60 °C for 4 h.

Table 1
Physicochemical properties of fly ash.

Chemical composition (wt.%)							
SiO_2	Al_2O_3	Fe_2O_3	CaO	MgO	Na_2O	K_2O	LOI[a]
60.48	28.15	4.52	1.71	0.47	0.14	1.41	1.59

Physical properties	
Glass content, %	43
Mineral phases	Quartz, mullite

[a] Loss on ignition.

3. Results and discussion

3.1. Characterisation of vibratory milled fly ash

EVM due to the eccentric drive generates 5-axis elliptical, circular and linear vibrations. This results in a very significant intensification of the impact forces/milling energy leading to efficient milling and mechanical activation [23–26]. Fig. 1

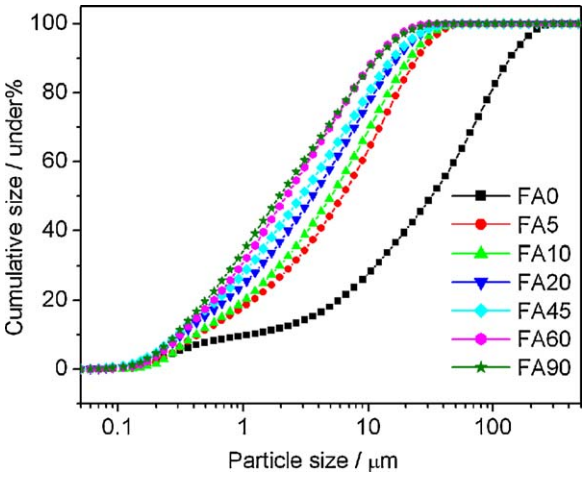

Fig. 1. Particle size distribution of raw and vibratory milled fly ash. The cumulative particle size distribution is plotted.

Table 2
Characteristic particle diameters and specific surface area of fly ash milled for different time.

Milling time (min)	d_{10}	d_{50}	d_{90}	Specific surface area (m^2/g)
0	1.28	37.73	158.49	0.969
5	0.51	7.23	28.59	1.439
10	0.49	5.88	24.99	1.502
20	0.38	4.17	19.72	1.781
30	0.37	3.82	18.43	2.065
45	0.35	3.4	18.28	2.316
60	0.35	2.57	14.26	2.333
90	0.34	2.27	13.62	2.57

shows typical cumulative particle size distribution of fly ash milled for different time in EVM. The characteristic particle diameters and specific surface area as a function of milling time are given in Table 2. The particle size reduction was more during initial 10 min which gradually decreased with milling time. The morphology of the raw fly ash and fly ash milled for 30 min is given in Fig. 2a and b respectively. The FA0 contained mostly spherical cenosphere ranging in size from 2 to 20 μm. After milling large sized cenospheres are broken into irregular shaped particles and those with size <5 μm mostly retained their original spherical shape. XRD patterns of the samples are given in Fig. 3. XRD patterns indicated no apparent change in the mineralogy and peak intensities in the samples milled up to 60 min, however, a slight decrease in peak intensity and broadening of quartz and mullite was detected in the sample milled for 90 min (Fig. 3). This is due to the damage of crystalline structure during intense milling which resulted into micro stress and peak broadening [15–17]. The IR spectra in Fig. 4 show subtle structural changes due to milling. The milling results in a change in the intensity of IR peaks corresponding to Si–O–Si bending (460 cm^{-1}), T–O–Si (T = Si, Al) and asymmetric stretching (913, 1090 and 1160 cm^{-1}). The Si–O–Si symmetric stretching band observed at 798 cm^{-1} and which was nearly absent in the FA0 appeared after the milling and its intensity increased in FA5 and FA60 with increase in milling time (Fig. 4) [26,27]. The XRD results (Fig. 3) and IR spectra (Fig. 4) indicate that the effect of milling on fly ash extends beyond creation of new surface due to particle breakage and it undergoes structural changes and mechanical activation [15–17].

3.2. Calorimetric studies of geopolymerisation of vibratory milled fly ash

The key processes occurring during geopolymerisation are dissolution, precipitation, gel formation, restructuring and polymerisation and hardening [27]. To study the effect of mechanical activation on above geopolymerisation mechanism, isothermal conduction calorimeter was used under following two conditions: (a) at ambient temperature (27 °C), and (b) at 60 °C.

Fig. 5 shows the rate of heat evolution (dq/dt) at 27 °C for different milling time. The first peak (which appears more like a straight line) in the beginning corresponds to wetting and partial dissolution of glassy content followed by small induction period as a consequence of low reactivity [28]. The second exothermic peak after induction period is associated with dissolution–precipitation reaction; mainly formation of hydrated alumino-silicate gel [27]. The peak maxima shifted towards lower time and its intensity increased with an increase in milling time indicating increased reactivity of fly ash and consequently enhanced dissolution–precipitation reaction [27,29]. The most interesting feature was beginning of a third exothermic peak after 32 h in the FA45 that becomes more prominent in FA60 and FA90 respectively. This low intensity peak is attributed to geopolymerisation. In the earlier studies [30,31], developments of strength due to ambient temperature

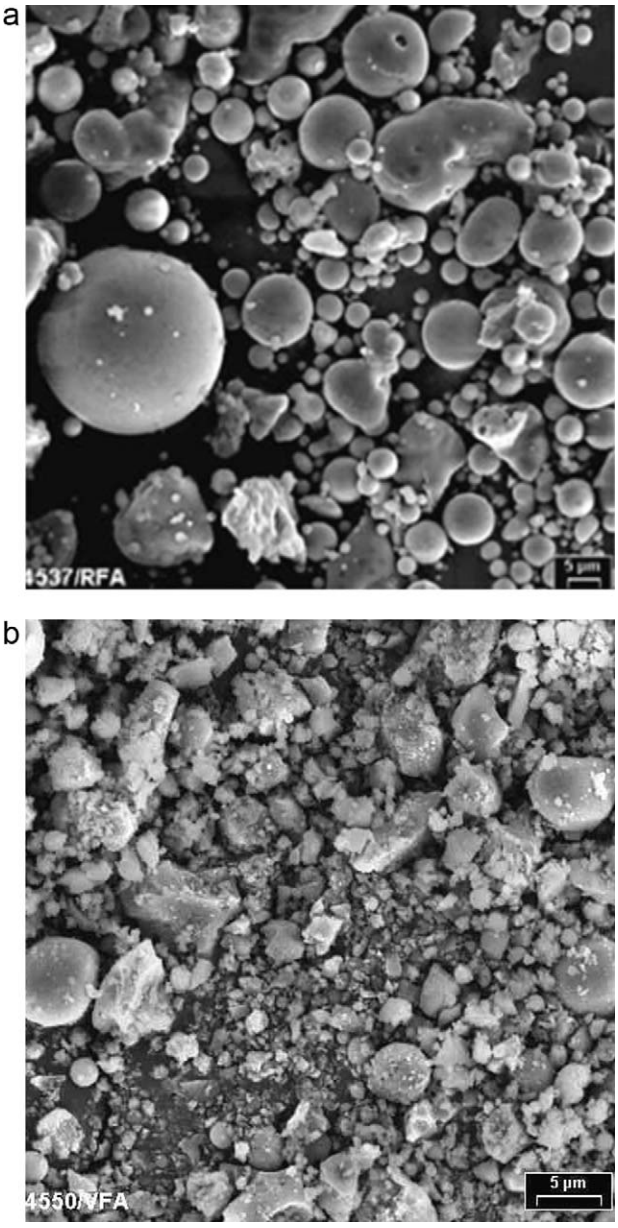

Fig. 2. (a) Morphology of raw fly ash (FA0) showing spherical cenosphere of various sizes. (b) Morphology of fly ash vibratory milled for 30 min showing presence of both angular and spherical particles with aggregation.

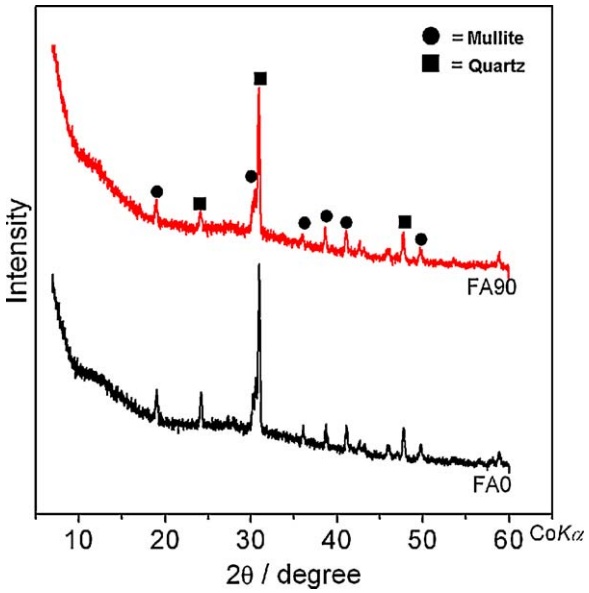

Fig. 3. XRD result of FA0 and FA90. FA90 samples show a minor decrease in peak intensity of quartz and mullite.

geopolymerisation were reported but calorimetric evidence of geopolymerisation of mechanically activated fly ash was observed for the first time. Initiation of geopolymerisation at 27 °C may be attributed to relaxation of mechanical energy stored in fly ash particles due to mechanical activation [15–17].

Fig. 6 shows the rate of heat evolution (dq/dt) at 60 °C for the samples milled for different time. In this case, only one peak corresponding to geopolymerisation was observed [20]. Similar to the results at 27 °C, the maximum rate of heat evolution [$(dq/dt)_{max}$] increased and time at which peak maxima (t_{max}) occurred shifted to lower time with increase in milling time. The prominent trend at 60 °C was due to the combined effect of thermal and mechanical activation which accelerated the geopolymerisation reaction. The quantity [$(dq/dt)_{max}$] was taken as a measure of fly ash reactivity. It was found that fly ash reactivity varies non-linearly with median particle size (d_{50}) (Fig. 7). The reactivity increases vary rapidly when the particle size is reduced to less than 5–7 μm. This value corresponds to

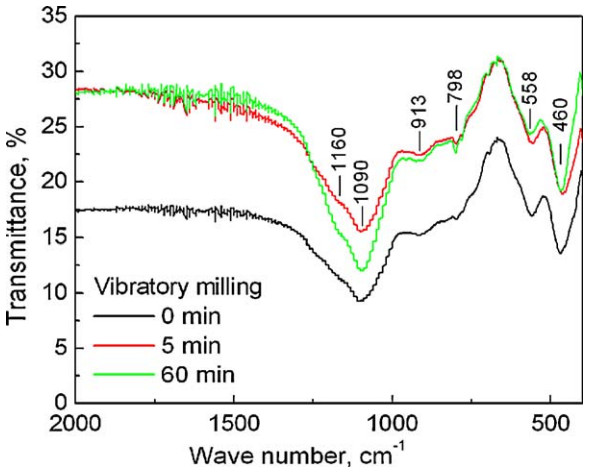

Fig. 4. FTIR spectra of fly ash vibratory milled for 0, 5 and 60 min.

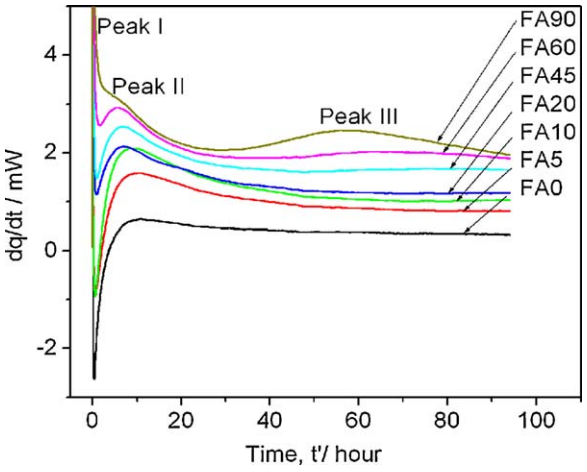

Fig. 5. Isothermal conduction calorimetry showing rate of heat evolution (dq/dt) at 27 °C of the samples milled for different time.

critical size for silicates below which mechanical activation begins to manifest [16].

3.3. Physical properties of geopolymer

The physical properties were measured as follows:

(a) setting time at 27 °C
(b) compressive strength of cast samples after curing for 28 days
(c) compressive strength of samples after the casting and curing of samples at 27 °C for 24 h and geopolymerisation at 60 °C for 4 h

Fig. 8 shows the variation of setting time for the samples milled for different time. The FA0 samples took long time (285 min) to set. A gradual decrease in setting time with milling duration is observed. Compressive strength of the samples after ambient temperature (27 °C) curing and elevated temperature

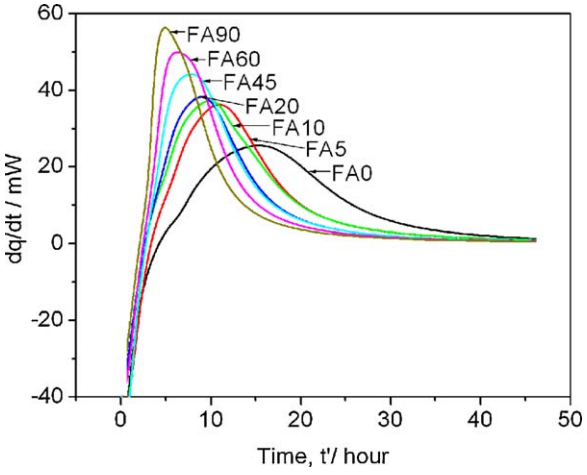

Fig. 6. Isothermal conduction calorimetry showing rate of heat evolution (dq/dt) during geopolymerisation at 60 °C of the samples milled for different time.

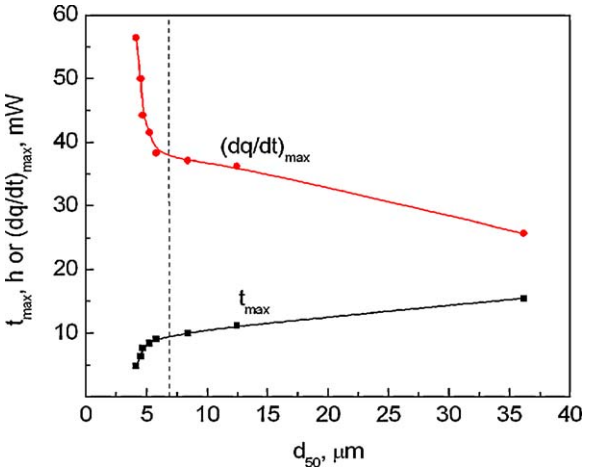

Fig. 7. Effect of particle size on the reactivity of fly ash. The quantity [$(dq/dt)_{max}$] was taken as a measure of fly ash reactivity.

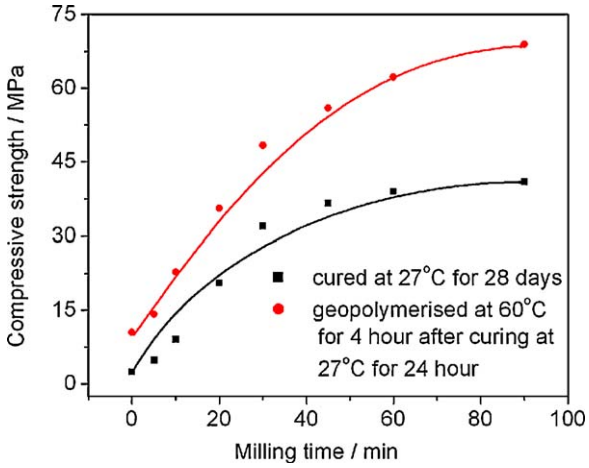

Fig. 9. Variation of compressive strength of the samples milled for different time and cured at 27 °C and 60 °C.

(60 °C) geopolymerisation is given in Fig. 9. In both the cases, compressive strength improved with milling time, however, the compressive strength values were higher in the samples cured at elevated temperature.

3.4. Correlation between physical properties of geopolymer and fly ash reactivity

An attempt was made to correlate the properties of geopolymer samples with mechanically induced reactivity of fly ash. Fig. 10 shows the variation of setting time (27 °C) and compressive strength (at 27 °C and 60 °C) with reactivity of fly ash. The variation of reactivity with inverse of median size (i.e. $1/d_{50}$; a measure of relative specific surface area) is also included in the figure to further elucidate the correlation between different parameters. A more detailed analysis indicated that geopolymer property (P) can be correlated with $1/d_{50}$ by the following expression:

$$\ln\left(\frac{P_{(FAt)}}{P_{(FA0)}}\right) = A + B\left(\frac{1}{d_{50}}\right) \quad (1)$$

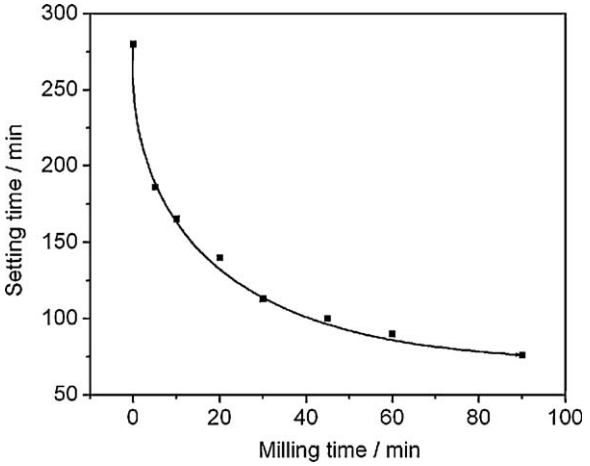

Fig. 8. Variation of setting time for the samples milled for different time.

where P_{FAt} and P_{FA0} are the value of property (P) for different milling time 't' (t = 5, 10, 15,. . ., 90, etc.) and initial value (t = 0); A and B are constant). The values of parameter A and B and correlation coefficient (R) are given in Table 3. High correlation coefficient values (Table 3) indicate that particle size has an important effect on setting time and strength development.

3.5. Characterisation of geopolymer samples

3.5.1. FTIR studies

Fig. 11 shows the FTIR spectra of selected geopolymer matrixes. The bands at 460 cm^{-1} was related to Al–O/Si–O in plane and bending modes, 730 cm^{-1} with octahedral Al, 820 cm^{-1} with tetrahedral Al–O stretching and, 900–1030 cm^{-1} with asymmetric Al–O/Si–O stretching [32,33]. The change in intensity of peaks was associated with the structural reorganisation due to MA [26]. In the geopolymer samples prepared using mechanically activated fly ash, there is an increase in the intensity of IR peaks indicating greater polymerisation. The O–H stretching bands (3440, 2930 cm^{-1}) does not show a well defined trend with milling time even though the intensity of IR peak in FA0 was higher than FA90. Higher peak intensity signifies greater incorporation of molecular water in FA0 than FA90.

The IR peak around 1000 cm^{-1} is the result of overlapping of IR peaks related to SiQ^n (n = 0–4) structural units [34–39]. The peak around 1090 cm^{-1} and the shoulder around 1160 cm^{-1} existing in all mechanical activated materials prior their geopolymerisation indicate the predominance of SiQ^n (n = 3–4) structural units (mainly sheet structure) over the SiQ^n (n = 0–2) ones (mainly chain structure). The splitting can be explained as follows: dissolution caused depolymerisation forming a less polymerised structure SiQ^n (n = 2) and creating the peak around 997 cm^{-1} (this is observed also in SEM photos where fibres are present). At the same time, the initial non-dissolved high polymerised structures SiQ^n (n = 3–4) were resolved giving rise to the clear peak at 1091 cm^{-1}.

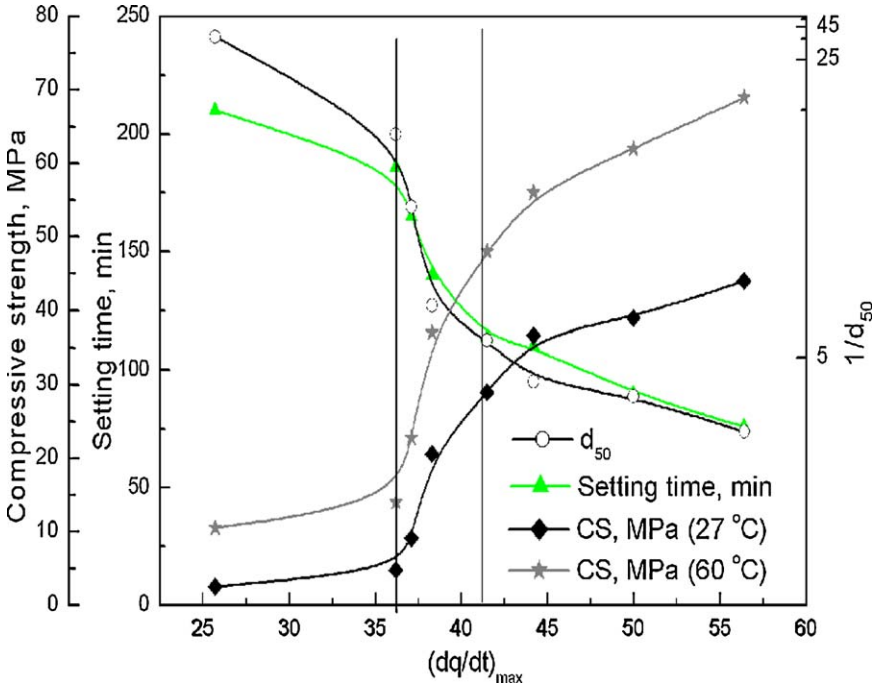

Fig. 10. Variation of setting time (27 °C) and compressive strength (at 27 °C and 60 °C) with reactivity of fly ash.

3.5.2. Microstructural studies

Fig. 12 shows the XRD patterns of geopolymers derived from raw and mechanically activated fly ash. For all the studied samples, the intensity of quartz and mullite peaks was decreased with milling time. This decrease is related to the higher reactivity of fly ash which resulted into consumption of quartz and mullite phase. In addition, low intensity diffraction peaks of phases such as sodalite at 27°, 42° and 46° and chabazite at 25°, 33° and 36° were present as product of geopolymerisation [8].

Fig. 13(a–d) shows the microstructure of selected geopolymer samples cured at 60 °C. In general, the compactness of microstructure improved with duration of mechanical activation which may be explained by the formation of greater amount of alumino-silicate gel. In FA0 samples, partially reacted cenosphere with presence of reaction product on the

Table 3
Values of parameters A and B and correlation coefficient (R) for Eq. (1).

Property (P)	A	B	R
Setting time	0.230	−4.542	−0.95
Compressive strength at 27 °C	−0.409	14.305	0.99
Compressive strength at 60 °C	−0.346	9.452	0.99

The unit d_{50} is μm.

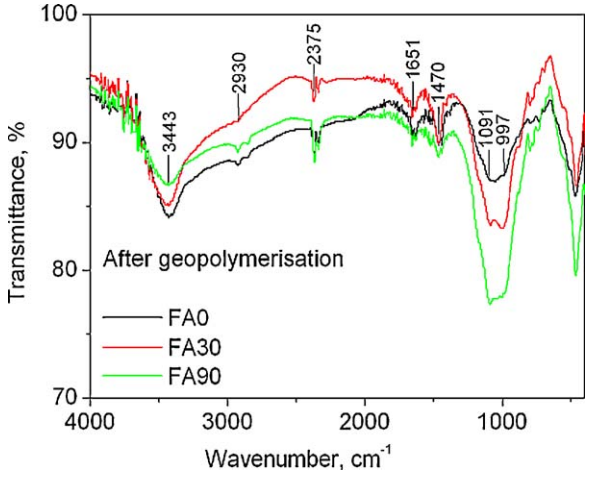

Fig. 11. FTIR spectra of select geopolymer samples. The effect of milling time is visible on Si–O(Al) stretching vibrations in SiO_4 tetrahedra near between 980 and 1100 cm^{-1}.

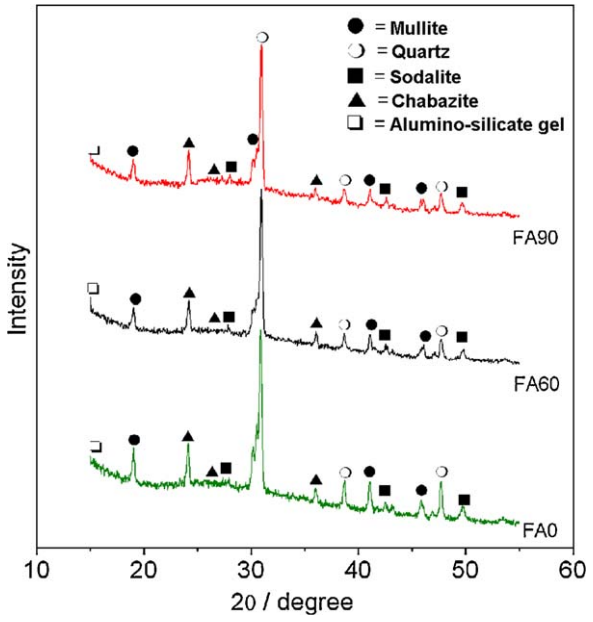

Fig. 12. XRD patterns of geopolymers derived from raw and mechanically activated fly ash.

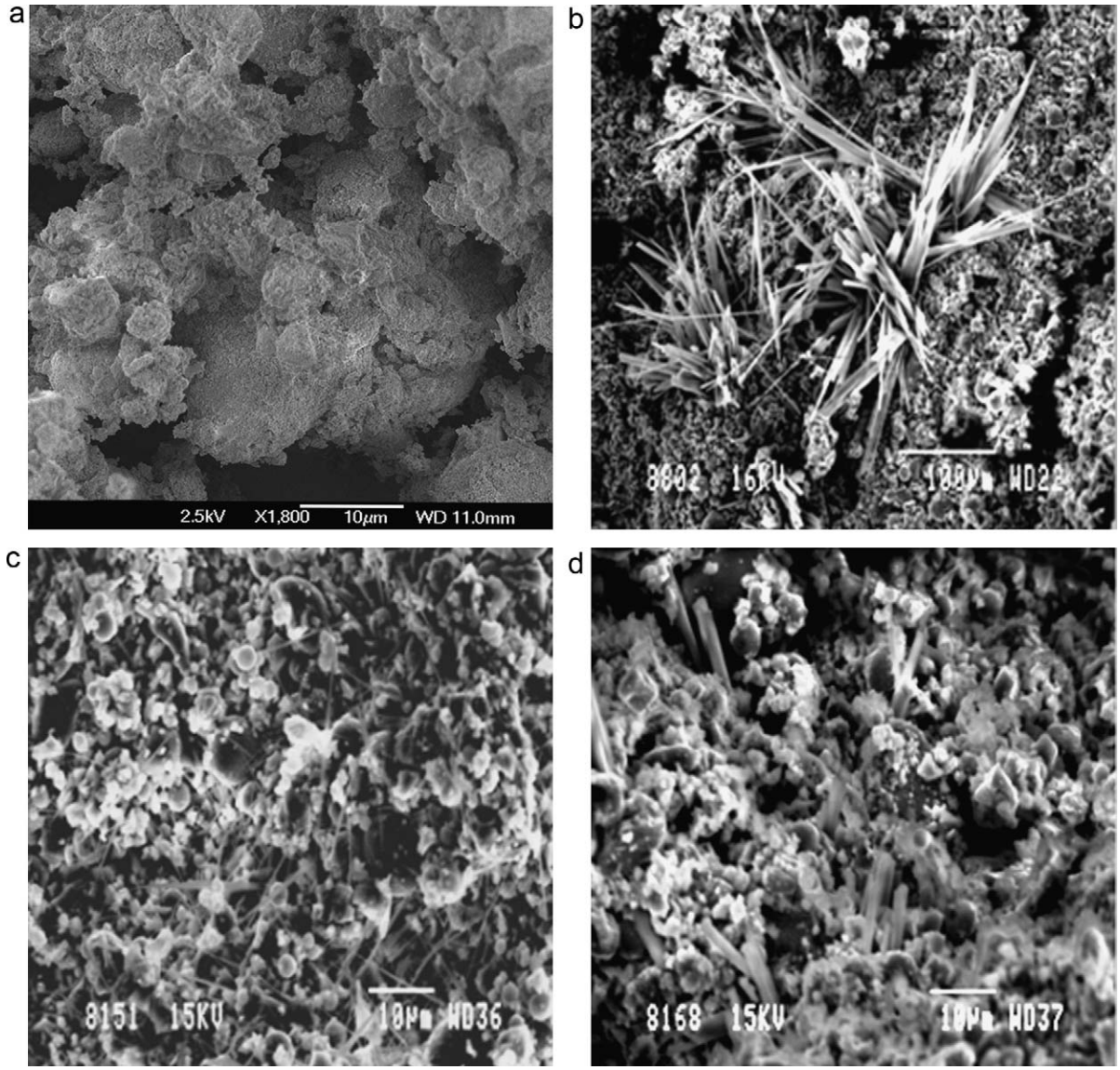

Fig. 13. (a) SEM of RFA showing partly reacted cenosphere. (b) SEM of FA30 geopolymer showing presence of radiating acicular structure. (c) SEM of FA60 showing long gel fibres. (d) SEM of FA90 showing compact structure and presence of tabular type of features with diffused boundary.

surface were main feature (Fig. 13a). With mechanical activation, the change in microstructure in terms of new morphological features, reaction products and compactness was distinctly evident. In general, following major morphological features were observed, partly reacted cenosphere (Fig. 13a), acicular shaped grains radiating from one place (Fig. 13b) fibrous products (Fig. 13c), and tabular type particles with no sharp geometric outline (Fig. 13d). Presence of gel was common in all the samples. EDS study of these morphological features was carried out and the analysis results are summarised in Table 4. The reaction product on the surface of cenosphere and gel product were

Table 4
Summary of microstructural features obtained using SEM-EDS.

	Composition	EDS summary	Remarks
1	Partially reacted cenosphere with crust on surface	Si/Al = ∼1.3–1.8, Si/Na = ∼0.15–0.4	Alumino-silicate hydrate with Na in structure
2	Gel phase	Si/Al = ∼2, Si/Na = ∼0.4–0.9	Alumino-silicate hydrate with Na in structure
4	Long acicular crystal	Si/Al = ∼2.5, Si/Na = ∼0.2–0.3	Corresponds to Na zeolite
5	Fibrous structure	Si/Al = ∼2.2, Si/Na = ∼0.2–0.4	Corresponds to Na zeolite

alumino-silicate hydrate gel with Na in structure. The change in microstructural features such as lowering of peak intensity of mullite and quartz, new morphological features, reaction products and increased compactness was due to the enhanced geopolymerisation reactions. Formation of acicular and fibrous features with composition corresponding to zeolite and presence of phases like sodalite and chabazite was due to the partial conversion of geopolymer gel into zeolite [40,41].

The alteration in geopolymerisation reactions was due to combined effect of particle size (increase in surface area) and change in reactivity due to mechanical activation. The intrinsic structure developed due to geopolymerisation at ambient and elevated temperature resulted into improvement in physical properties.

It is necessary to mention here that ambient temperature geopolymerisation induced by mechanical activation may not be a cheaper substitute of thermal treatment at 60 °C. But it may prove a feasible alternative as providing thermal treatment (60–100 °C for few hours) for geopolymerisation at construction site is a difficult proposition.

4. Conclusions

The major conclusions of this study are:

1. Mechanical activation in eccentric vibratory mill increases the reactivity of fly ash. The reactivity of fly ash varies with median particle size and increases vary rapidly when the particle size is reduced to less than 5–7 μm. As a result, geopolymerisation at ambient temperature is possible.
2. The effect of mechanical activation on structural reorganisation is evident from FTIR spectrum corresponding to Si–O stretching. The splitting of peak is associated with formation of less polymerised structure at 997 cm^{-1} and non-dissolved high polymerised structures at 1091 cm^{-1}.
3. A high degree of correlation between the properties of geopolymer (setting time and compressive strength) and inverse of median size of fly ash is observed.
4. Combined effect of particle size (increase in surface area) and change in reactivity due to mechanical activation altered the geopolymerisation reaction. The improvement in physical properties is related to the intrinsic structure developed due to enhanced geopolymerisation.

Acknowledgements

The authors are grateful to Director, National Metallurgical Laboratory, Council for Scientist & Industrial Research, Jamshedpur, India for his kind permission to publish the paper. Authors would like to acknowledge the characterisation support from Dr. T. Mishra, Mr. B. Mahato and Mr. M. Gunjan. The fly ash used in the study was received from Grasim Cement, Rawan, Chattisgarh (India) and is gratefully acknowledged.

References

[1] J. Davidovits, Geopolymers and geopolymeric materials, J. Therm. Anal. 35 (1989) 429–441.
[2] M. Gordon, J.L. Bell, W.M. Kriven, Comparison of naturally and synthetically derived, potassium-based geopolymers, Ceram. Trans 165 (2005) 95–106.
[3] H. Xu, J.S.J. Van Deventer, The geopolymerization of alumino-silicate minerals, Int. J. Miner. Process. 59 (2000) 247–266.
[4] H. Wang, H. Li, F. Yan, Synthesis and mechanical properties of metakaolinite-based geopolymer, Colloids Surf. A: Physicochem. Eng. Aspects 268 (2005) 1–6.
[5] P. Duxson, S.W. Mallicoat, G.C. Lukey, W.M. Kriven, J.S.J. Van Deventer, The effect of alkali and Si/Al ratio on the development of mechanical properties of metakaolin-based geopolymers, Colloids Surf. A: Physicochem. Eng. Aspects 292 (2007) 8–20.
[6] A. Palomo, M.W. Grutzeck, M.T. Blanco-Varela, Alkali activated fly ashes: a cement for the future, Cem. Concr. Res. 29 (1999) 1323–1329.
[7] J.C. Swanepoel, C.A. Strydom, Utilisation of fly ash in a geopolymeric material, Appl. Geochem. 17 (2002) 1143–1148.
[8] T. Bakharev, Durability of geopolymer materials in sodium and magnesium sulfate solutions, Cem. Concr. Res. 35 (2005) 1233–1246.
[9] B.V. Rangan, D. Hardjito, S.E. Wallah, D.M.J. Sumajouw, Studies on fly ash based geopolymer concrete, in: J. Davidovits (Ed.), Proceedings of 4th World Congress on Geopolymer, Saint Quentin, France, 2005, pp. 133–137.
[10] A. Fernandez-Jimenez, A. Palomo, Characterisation of fly ashes. Potential reactivity as alkaline cements, Fuel 82 (2003) 2259–2265.
[11] F. Skvara, J. Bohunek, Chemical activation of substances with latent hydraulic properties, Ceram. Silik. 43 (1999) 111–116.
[12] A. Puri, A. Badanoiu, G. Voicu, Eco-Friendly binders based on fly ash, Rev. Roum. Chim. 53 (2008) 1069–1076.
[13] J.G.S. Van Jaarsveld, J.S.J. Van Deventer, Effect of the Alkali metal activator on the properties of fly ash-based geopolymers, Ind. Eng. Chem. Res. 38 (1999) 3932–3941.
[14] Y. Fan, S. Yin, Z. Wen, J. Zhong, Activation of fly ash and its effects on cement properties, Cem. Concr. Res. 29 (1999) 467–472.
[15] V.V. Boldyrev, Mechanochemistry and mechanical activation of solids, Russ. Chem. Rev. 75 (2006) 177–189.
[16] P. Balaz, Mechanochemistry, Nanoscience and Minerals Engineering. Springer Publication, XIV, 2008.
[17] A.J. Juhasz, L. Opoczky, Mechanical activation of Minerals by Grinding: Pulverizing and Morphology of Particles, Ellis Horwood Limited, NY, 1994
[18] R. Kumar, S. Kumar, S. Badjena, S.P. Mehrotra, Hydration of mechanically activated granulated blast furnace slag, Met. Trans. B 36 (2005) 873–883.
[19] S. Kumar, R. Kumar, A. Bandopadhyay, T.C. Alex, B. RaviKumar, S.K. Das, S.P. Mehrotra, Mechanical activation of granulated blast furnace slag and its effect on the properties and structure of portland slag cement, Cem. Concr. Comp. 8 (2008) 679–685.
[20] S. Kumar, R. Kumar, T.C. Alex, A. Bandopadhyay, S.P. Mehrotra, Influence of reactivity of fly ash on geopolymerisation, Adv. Appl. Ceram. 106 (2007) 120–127.
[21] S. Kumar, R. Kumar, T.C. Alex, A. Bandopadhyay, S.P. Mehrotra, Effect of mechanically activated fly ash on the properties of geopolymer cement, in: J. Davidovits (Ed.), Proceedings of 4th World Congress on Geopolymer, Saint Quentin, France, 2005, pp. 113–116.
[22] J. Temuujin, R.P. Williams, A. van Riessen, Effect of mechanical activation of fly ash on the properties of geopolymer cured at ambient temperature, J. Mater. Process. Technol. 209 (2009) 5276–5280.
[23] E. Gock, W. Beenken, M. Gruschka, US Patent 5570848, (1996), Eccentric vibrating mill.
[24] E. Gock, K.E. Kurrer, Eccentric vibratory mills—theory and practice, Powder Technol. 105 (1999) 302–310.
[25] S. Kumar, R. Kumar, A. Bandopadhyay, Innovative methodologies for the utilisation of metallurgical and other wastes, Resour. Conserv. Recy. 48 (2006) 301–314.
[26] R. Kumar, S. Kumar, S.P. Mehrotra, Towards sustainable solutions for fly ash through mechanical activation, Resour. Conserv. Recy. 52 (2007) 157–179.
[27] P. Duxson, A. Fernandez-Jimenez, J.L. Provis, G.C. Lukey, A. Palomo, J.S.J. Van Deventer, Geopolymer technology: the current state of the art. Advances in geopolymer science and technology, J. Mater. Sci. 42 (2007) 2917–2933.

[28] A. Buchwald, R. Tatarin, D. Stephan, Reaction progress of alkaline-activated metakaolin-ground granulated blast furnace slag blends, J. Mater. Sci. 44 (2009) 5609–5617.
[29] M.L. Granizo, M.T. Blanco-Verela, A. Palomo, Influence of the starting kaolin on alkali-activated materials based on metakaoline—study of the reaction parameters by isothermal conduction calorimetry, J. Mater Sci. 35 (2000) 6309–6315.
[30] M.L. Granizo, S. Alonso, M.T. Blanco-Verela, A. Palomo, Alkaline activation of metakaolin: effect of calcium hydroxide in the products of reaction, J. Am. Ceram. Soc. 85 (2002) 225–231.
[31] P.S. Singh, M. Trigg, I. Burgar, T. Bastow, Structural studies of geopolymers by ^{29}Si and ^{27}Al MAS-NMR, Mater. Sci. Eng. A 396 (2005) 392.
[32] A. Palomo, F.P. Glasser, Chemically-Bonded cementitious material based on metakaolin, Br. Ceram. Trans. J. 91 (1992) 107–112.
[33] J.W. Phair, J.S.J. Van Deventer, J.D. Smith, Mechanism of polysialation in the incorporation of zirconia into fly ash-based geopolymers, Ind. Eng. Chem. Res. 39 (2000) 2925–2934.
[34] M.Y.A. Mollah, T.R. Hess, D.L. Cocke, Surface and bulk studies of leached and unleached fly ash using XPS, SEM, EDS and FTIR techniques, Cem. Concr. Res. 24 (1994) 109–118.
[35] D. Dimas, I. Giannopoulou, D. Panias, Polymerization in sodium silicate solutions: a fundamental process in geopolymerization technology, J. Mater. Sci. 44 (2009) 3719–3730.
[36] I. Lecomte, C. Henrist, M. Liegeois, F. Maseri, A. Rulmont, R. Cloots, (Micro)-structural comparison between geopolymers, alkali-activated slag cement and Portland cement, J. Eur. Ceram. Soc. 26 (2006) 3789–3797.
[37] M. Sitarz, M. Handke, W. Mozgawa, Identification of silicooxygen rings in SiO_2 based on IR spectra, Spectrochim. Acta Part A: Mol. Biomol. Spectrosc. 56 (2000) 1819–1823.
[38] H. Rahier, W. Simons, B. Van Mele, M. Biesemans, Low-temperature synthesized aluminosilicate glasses: Part III influence of the composition of the silicate solution on production, structure and properties, J. Mater. Sci. 32 (1997) 2237–2247.
[39] W.K.W. Lee, J.S.J. van Deventer, Use of infrared spectroscopy to study geopolymerization of heterogeneous amorphous aluminosilicates, Langmuir 19 (2003) 8726–8734.
[40] T. Bakharev, Thermal behaviour of geopolymers prepared using class f fly ash and elevated temperature curing, Cem. Concr. Res. 36 (2006) 1134–1147.
[41] B. Zhang, K.Z.D. MacKenzie, I.W.M. Brown, Crystalline phase formation in metakaolinite geopolymers activated with NaOH and sodium silicate, J. Mater. Sci. 44 (2009) 4668–4746.